ChemPubSoc Europe

DOI: 10.1002/chem.201504780

CHEMISTRY A European Journal Full Paper

Radical Cyclisation

Radical Cyclisation of α-Halo Aluminium Acetals: A Mechanistic Study

Romain Bénéteau,[a] Anne Boussonnière,[a] Jean-Christophe Rouaud,[a] Jacques Lebreton,[a] Jérôme Graton,[a] Denis Jacquemin,[a, b] Muriel Sebban,[c] Hassan Oulyadi,[c] Ghanem Hamdoun,[c] Amber N. Hancock,[d] Carl H. Schiesser,[d] and Fabrice Dénès*[a]

Dedicated to Professor Jean-François Normant on the occasion of his 80th birthday.

Abstract: α-Bromo aluminium acetals are suitable substrates for Ueno–Stork-like radical cyclisations affording γ-lactols and acid-sensitive methylene-γ-lactols in high yields. The mechanistic study herein sets the scope and limitation of this reaction. The influence of the halide (or chalcogenide) atom X (X = Cl, Br, I, SPh, SePh) in the precursors α-haloesters, as well as influence of the solvent and temperature was studied. The structure of the aluminium acetal intermediates resulting from the reduction of the corresponding α-haloesters has been investigated by low-temperature ^{13}C-INEPT diffusion-ordered NMR spectroscopy (DOSY) experiments and quantum calculations, providing new insights into the structures of these thermally labile intermediates. Oxygen-bridged dimeric structures with a planar Al_2O_2 ring are proposed for the least hindered aluminium acetals, while monomeric structures seem to prevail for the most hindered species. A comparison against the radical cyclisation of aluminium acetals derived from allyl and propargyl alcohols with the parent Ueno–Stork has been made at the BHandHLYP/6-311++G(d,p) level of theory, highlighting mechanistic similarities and differences.

Introduction

Aluminium acetals are long-known intermediates in the reduction of esters to aldehydes or alcohols with aluminium hydrides. These species are thermally labile, but those resulting from a reduction with diisobutylaluminium hydride (DIBAL-H) proved to be sufficiently stable at low temperature to be quenched to give either aldehydes (acidic quenching) or mixed acetals (e.g., trapping with an acylating agent).[1] We previously reported the use of these intermediates for the first time in a radical reaction. We showed that aluminium acetals resulting from the reduction of α-bromoesters with DIBAL-H were stable enough at temperatures below −70 °C to engage in a radical cyclisation in the presence of nBu$_3$SnH, initiated with Et$_3$B/air. The process was high yielding with most of the α-bromo precursors and gave access to γ-lactols[2] and to highly acid-sensitive methylene-γ-lactols.[3] One of the main advantages of this reaction compared to the classical Ueno–Stork reaction,[4,5] which uses α-haloacetals as the precursors for the radical cyclisation, is that it allows for a direct access to γ-lactols or lactones without the need for strongly acidic conditions. In that sense, it complements nicely the Ueno–Stork reaction, which gives access to cyclic acetals, for which the reactive aldehyde functionality is protected as an acetal, thus offering the possibility to pursue further functionalisation elsewhere on the molecule. The aluminium acetals resulting from the cyclisation process are reactive intermediates that could be oxidised by simple aldehydes to produce γ-lactones[6] and polysubstituted butenolides.[7] So far no mechanistic study has been reported. The structure of the aluminium acetal intermediates of both the α-halo radical precursor and the radical species that undergoes radical cyclisation are totally unknown. In order to get some insights into the reaction mechanism of this reaction, we conducted a systematic study that allowed us to highlight the subtle differences in reactivity between different types of precursors. Indeed, for similar structures of the α-haloesters used as precursors for the preparation of the aluminium acetals, the yields obtained in γ-lactols strongly depended upon the nature of the halide or chalcogenide, the solvent,

[a] R. Bénéteau, A. Boussonnière, J.-C. Rouaud, Prof. Dr. J. Lebreton, Dr. J. Graton, Prof. Dr. D. Jacquemin, Dr. F. Dénès
CEISAM UMR 6230 - UFR des Sciences et des Techniques
Université de Nantes, 2 rue de la Houssinière BP
92208-44322 Nantes Cedex 3 (France)
E-mail: fabrice.denes@univ-nantes.fr

[b] Prof. Dr. D. Jacquemin
Institut Universitaire de France, 1, rue Descartes
75231 Paris Cedex 05 (France)

[c] Dr. M. Sebban, Prof. Dr. H. Oulyadi, G. Hamdoun
Normandie Université, COBRA UMR6014 and FR3038, Université de Rouen; INSA de Rouen; CNRS,
76821 Mont-Saint-Aignan Cedex (France)

[d] Dr. A. N. Hancock, Prof. Dr. C. H. Schiesser
School of Chemistry and
Bio21 Molecular Science and Biotechnology Institute
The University of Melbourne, Victoria, 3010 (Australia)

Supporting information and ORCIDs for the authors for this article is available on the WWW under http://dx.doi.org/10.1002/chem.201504780

and the temperature. Using both experimental (synthetic and low-temperature NMR studies) and computational methods in parallel, we were able to get useful information regarding the plausible structures of these thermally labile intermediates. Preliminary experiments highlighted a stark difference in the radical cyclisation step between some precursors, and quantum calculations indicate agreement. A comparison with the classical Ueno–Stork reaction, which relies on the use of classical α-haloacetals, is also presented. Quantum calculations have been conducted for both the classical Ueno–Stork cyclisation and the radical cyclisation of aluminium acetals and transition states were located at the BHandHLYP/6-311++G(d,p) level of theory, allowing for a direct comparison between the two systems. These results are presented herein.

Results and Discussion

We have chosen a model substrate for our study, with minimal variation of the structure in order to exclude the effect of side chain, and focus only on the influence of the substitution at the α-position on the ester moiety. The variations in the structures were thus limited to the nature of the halide (or chalcogenide) and the number of alkyl substituents at the carbon atom at the α-position. The general structure of these substrates is shown in Scheme 1. The reaction conditions were identical for all reactions, unless otherwise stated. Although other factors may interfere in the cyclisation process, the yields of the isolated products are likely to give indirect information on the stability of the aluminium acetal intermediates.

We first decided to screen possible solvents for this radical reaction. Protic solvents were not tested, as the first step requires the use of an aluminium hydride. The feasibility of the overall sequence was tested in toluene, methylene chloride, and *n*-hexane. Preliminary experiments indicated that both toluene and methylene chloride were suitable solvent for this radical cyclisation (Table 1, entries 1 and 2). The yields in *n*-hexane dropped to 55%, presumably due to the poor solubility of both the precursor and the aluminium acetal in this solvent at low temperature (Table 1, entry 3). We therefore decided not to further investigate this solvent, although it might be useful in combination with other non-protic solvents to reach temperatures below −80 °C, which might be beneficial in some cases for stability and diastereoselectivity. Polar solvents such as THF led to the decomposition of the aluminium acetal intermediate and, in this case, the alcohol resulting from over-reduction was the major compound formed (Table 1, entry 4).

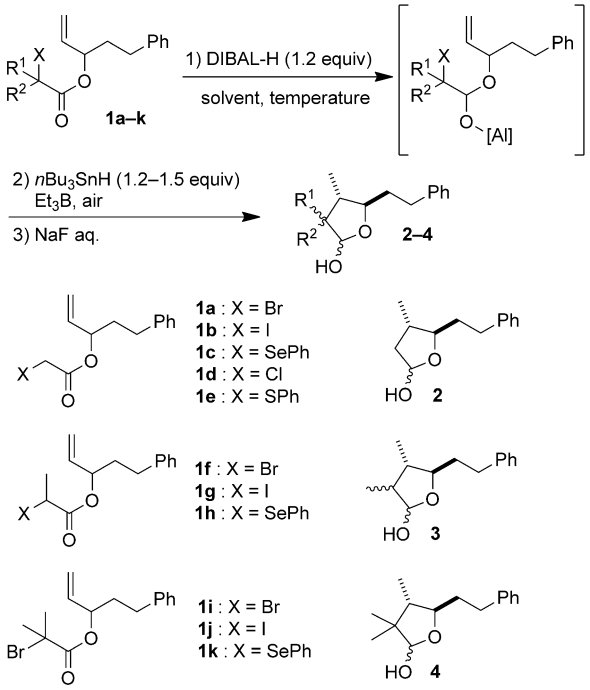

Scheme 1. General scheme for the cyclisation of aluminium acetals.

Table 1. Screening of solvent for the radical cyclisation.

Entry	Substrate[a]	Solvent	*T* [°C][b]	Product	Yield [%][c]
1	**1a**	toluene	−73	**2**	88±2
2	**1a**	CH_2Cl_2	−73	**2**	80±2
3	**1a**	*n*-hexane	−73	**2**	55
4	**1a**	THF	−73	**2**	0[d]

[a] All reactions were carried out at −73 °C on a 2 mmol scale (and repeated 2–3 times), using 1.2 equiv of DIBAL-H (solution in the same solvent as the solvent of reaction), 1.2–1.5 equiv of nBu_3SnH and 0.3–0.6 equiv of Et_3B (1 M solution in hexanes). [b] Temperature measured inside the reaction flask. [c] Yields in isolated product, after purification by chromatography on silica gel or Silica-KF. [d] Mainly over-reduction was observed.

Different reducing agents were tested in order to achieve the reduction of bromoesters into the corresponding tetrahedral intermediates. Among the various reducing agents tested, the best results were obtained with DIBAL-H, as the more reactive Red-Al® led only to the displacement of the halogen atom, whereas $LiBHEt_3$ gave non-reproducible results (Table 2, entries 1, 4 and 5).

In the case of $LiBHEt_3$, the hydride was well transferred to the carbonyl group, as indicated on thin layer chromatography (TLC) by the presence of the allylic alcohol corresponding to the reduction of bromoester **1a**, but the addition of nBu_3SnH and air did not lead to a clean conversion into lactol **2**. In this

Table 2. Screening of initiator for the radical cyclisation of **1a** at −73 °C in toluene.

Entry	Hydride[a]	Equiv	Solvent	Initiator	Yield [%][c]
1	DIBAL-H	1.2	toluene	Et_3B/air	90
2	DIBAL-H	2	toluene	Et_3B/air	91
3	DIBAL-H	3	toluene	Et_3B/air	88
4	Red-Al®[d]	1.1	toluene	Et_3B/air	0
5	$LiBHEt_3$[e]	1.1	toluene/THF	–/air	nd[f]

[a] All reactions were carried out at −73 °C on a 2 mmol scale (and repeated 2–3 times), using 1.2–1.5 equiv of nBu_3SnH and 0.6 equivalents of Et_3B (1 M solution in hexanes) and 2×1 mL of air (unless otherwise stated). [b] Temperature measured inside the reaction flask. [c] Yields in isolated product, after purification by chromatography on silica gel or Silica-KF. [d] 60 wt.% solution in toluene. [e] 1.0 M solution in THF. [f] Non-reproducible results.

case, no Et_3B was added since it should be released in the medium during the reduction step. We suspect in this case that the presence of THF present in the commercially available solution of $LiBHEt_3$ is responsible for the degradation of the aluminium acetal. This is in agreement with previous observations (Table 1, entry 4). The use of larger quantities of DIBAL-H gave very similar results to those obtained in the presence of only 1.2 equivalents, thus indicating that an excess of reducing agent does not significantly decrease the thermal stability of the acetal aluminium derived from **1a**, at least for reactions carried out in toluene at −73 °C (Table 2, entries 1–3).

We decided then to check whether initiators other than Et_3B/air could be used in this reaction. Et_2Zn and iBu_3Al gave very similar results to Et_3B in terms of yields (Table 3, entries 1–3), but the reactions seemed to be slightly faster. Interestingly, in the absence of any added initiator, the formation of γ-lactol **2** was still observed and, under otherwise similar reaction conditions, the product was isolated in about 50% (Table 3, entry 4). It is likely that homolytic cleavage of the carbon–aluminium bond in either the aluminium acetal intermediate or the remaining DIBAL-H (or both) occurred in the presence of air, and led to carbon-centred radicals that could initiate the radical chain.

Table 3. Screening of initiator for the radical cyclisation of **1a** at −73 °C in toluene.

Entry	Initiator[a]	Equiv[b]	Product	Yield [%][c]
1	Et_3B/air[d]	2×0.3	**2a**	90
2	Et_2Zn/air[e]	2×0.3	**2a**	87
3	iBu_3Al/air[f]	2×0.3	**2a**	91
4	–/air	–	**2a**	48±6
5	–/air[g]	–	**2a**	36
6	–/air[h]	–	**2a**	30

[a] All reaction were carried out at −73 °C on a 2 mmol scale (and repeated 2–3 times), using 1.2 equiv of DIBAL-H (solution in the same solvent as the solvent of reaction), 1.2–1.5 equiv of nBu_3SnH and 0.6 equivalent of Initiator and 2×1 mL of air (unless otherwise stated). [b] Temperature measured inside the reaction flask. [c] Yields in isolated product, after purification by chromatography on silica gel or Silica-KF. [d] 1 M solution in hexanes. [e] 15 wt.% in toluene. [f] 15 wt.% in toluene. [g] 2×20 mL of air. [h] Slow addition of 3×2 mL of air (over 11 h).

Modification of the amount and the rate of air introduced did not allow us to improve the yields (Table 3, entries 5 and 6), and accordingly the use of an initiator proved to be necessary in order to ensure high yields. The fact that the yields did not exceed 50% in the absence of initiator was somewhat puzzling and we suspect that the presence of an initiator, such as Et_3B, Et_2Zn or iBu_3Al, protects the air-sensitive aluminium acetals to some extent by consuming itself O_2 present in the medium, thus preventing a change in the structure of the aluminium acetals that seems to be detrimental to the thermal stability of the species.[8]

Screening the nature of the halide (or chalcogenide) revealed that only bromo, iodo and seleno derivatives (X = Br, I, and SePh) could be used as precursors for the radical cyclisation. Indeed, in the reaction with α-chloroester **1d** (Scheme 1) and α-phenylthio derivative **1e**, no traces of the corresponding γ-lactol **2** were observed. Because those derivatives are unlikely to undergo halogen (or chalcogen) abstraction by the tin-centred radical at −73 °C, the absence of reaction does not give any information concerning the thermal stability of the corresponding aluminium acetals. Nevertheless it allowed us to exclude the possibility that Lewis acids present in the medium (aluminium atoms) could facilitate the homolytic substitution in a way that would allow for the use of these less reactive precursors in this cyclisation process. We focused then our attention on substrates **1a–c**, and the related compounds **1f–k**, which differ only by the presence of one or two substituents, at the α-position. The results obtained at −73 °C in different solvents are collected in Table 4.

Table 4. Influence of the solvent and substitution on the reduction-cyclisation process.

Entry	Substrate[a]	Solvent	T [°C][b]	Product	Yield [%][c]
1	**1a**	toluene	−73	**2**	88±2
2	**1b**	toluene	−73	**2**	96±1
3	**1c**	toluene	−73	**2**	87±1
4	**1f**	toluene	−73	**3**	83±1
5	**1g**	toluene	−73	**3**	80±3
6	**1h**	toluene	−73	**3**	78±1
7	**1f**	CH_2Cl_2	−73	**3**	88
8	**1g**	CH_2Cl_2	−73	**3**	83
9	**1h**	CH_2Cl_2	−73	**3**	31±2
10	**1i**	toluene	−73	**4**	51±2
11	**1j**	toluene	−73	**4**	19±1
12	**1k**	toluene	−73	**4**	14±1

[a] All reactions were carried out at −73 °C on a 2 mmol scale (and repeated 2–3 times), using 1.2 equiv of DIBAL-H (solution in the same solvent as the solvent of reaction), 1.2–1.5 equiv of nBu_3SnH and 0.3–0.6 equiv of Et_3B (1 M solution in hexanes). [b] Temperature measured inside the reaction flask. [c] Yields in isolated product, after purification by chromatography on silica gel or Silica-KF.

When no alkyl substituent is present at the α-position (cf. Scheme 1), very similar yields were obtained in toluene regardless of the nature of the halide or chalcogenide (Table 4, entries 1–3). This indicates that the corresponding aluminium acetal intermediates do not present a marked difference in their thermal stability on the reaction time scale (5–8 h) at −73 °C. The same general trend was observed with compounds **1f–h**, which possess a single alkyl substituent at the α-position (Table 4, entries 4–6), although lactol **3** was obtained in slightly lower yields (ca. 78–83%) than for the corresponding lactol **2** (87–96%). Unexpectedly, slightly higher yields in lactol **3** were obtained from **1f** (X = Br) and **1g** (X = I) (88% and 83%, respectively) for the reactions carried out in CH_2Cl_2 (Table 4, entries 7 and 8, vs. entries 4 and 5), while a significant drop in the yield was observed in CH_2Cl_2 for selenyl derivative **1h** (X = SePh) (Table 4, entry 9).

Not surprisingly, compounds **1i–k** with two alkyl substituents at the α-position were more difficult to reduce into the corresponding aluminium acetals and the latter seem to be

much less stable than the less hindered aluminium acetals obtained from **1a–h**. Here again, a stark contrast was observed between the precursors, depending on the nature of the halide or chalcogenide, as illustrated by the yields obtained at −73 °C from **1i** (X = Br), **1j** (X = I) and **1k** (X = SePh) (Table 4, entries 10–12). Only bromoester **1i** led to the corresponding γ-lactol **4** in an acceptable 50% yield at −73 °C, while the iodo and phenylselenyl analogues **1j** and **1k** gave lactol **4** in very low yields (below 20%).

As expected, the general trend observed when varying the temperature was that an increase of the temperature resulted in lower yields (Table 5, entries 1–9). However, some differences were observed depending on the nature of the precursor. For instance, with compounds **1a–c**, which have no alkyl substituents at the α-position, the increase of the temperature from −73 °C to −40 °C, significantly decreases the reaction yield with **1a** and **1c** (X = Br and X = SePh, respectively), but much less with **1b** (X = I). Indeed, the reaction carried out at −40 °C led to γ-lactol **2** in about 65% yield from **1a** and **1c**, while a high yield of about 85% was still obtained from **1b** (Table 5, entries 1–3 vs. Table 4, entries 1–3). Surprisingly, the yields in γ-lactol **2** obtained at −20 °C from **1a** were much higher than those obtained from **1c**, and more reproducible than with **1b** (Table 5, entries 4–6).

Table 5. Influence of the temperature on the stability of the aluminium acetals.

Entry	Substrate[a]	Solvent	T [°C][b]	Product	Yield [%][c]
1	**1a**	toluene	−40	**2**	65 ± 1
2	**1b**	toluene	−40	**2**	85 ± 4
3	**1c**	toluene	−40	**2**	66 ± 2
4	**1a**	toluene	−20	**2**	30 ± 2
5	**1b**	toluene	−20	**2**	30 ± 25[d]
6	**1c**	toluene	−20	**2**	0
7	**1f**	toluene	−40	**3**	43 ± 1
8	**1g**	toluene	−40	**3**	41 ± 5
9	**1h**	toluene	−40	**3**	13 ± 1
10	**1f**	toluene	−20	**3**	12 ± 1
11	**1g**	toluene	−20	**3**	0
12	**1h**	toluene	−20	**3**	0
13	**1i**	toluene	−40	**4**	42 ± 2
14	**1j**	toluene	−40	**4**	0

[a] All reaction were carried out at −73 °C on a 2 mmol scale (and repeated 2–3 times), using 1.2 equiv of DIBAL-H (solution in the same solvent as the solvent of reaction), 1.2–1.5 equiv of nBu$_3$SnH and 0.3–0.6 equiv of Et$_3$B (1 M solution in hexanes). [b] Temperature measured inside the reaction flask. [c] Yields in isolated product, after purification by chromatography on silica gel or Silica-KF. [d] Non-reproducible results. The reaction has been repeated 6 times and yields varied between 5–55%.

Contrary to what was observed at −73 °C in toluene with precursors **1a–c** and **1f–h**, which gave the cyclised compounds in similar yields (87–96%, vs. 78–83%, respectively), the reactions carried out at −40 °C indicated that the aluminium acetals prepared from **1f–h** showed a lower thermal stability than those obtained from **1a–c** (Table 5, entries 7–9 vs. entries 1–3). Increasing further the reaction temperature led to lower yields from **1f–h**, and only traces of lactol **3** (if any) were obtained at −20 °C (Table 5, entries 10–12).

For the more hindered precursors **1i** and **1j** with two alkyl substituents at the α-position, only the reaction carried out from **1i** (X = Br) led to lactol **4** (Table 5, entries 13 and 14).

From this study it appeared that both the substituents at the α-position and the nature of the halide (or chalcogenide) play a significant role on the stabilisation of the thermally labile aluminium acetal intermediates. Moreover, although probably innocent in the radical cyclisation itself, the solvent also proved to play a role in this reaction. At this stage, all these effects were difficult to rationalise and we decided to have a look at the structure of the aluminium acetal intermediates.

Conformational analysis and structure of the aluminium acetals

DFT geometry optimisations at the PCM(toluene)-B3LYP/6-31 + G(d,p) level were carried out on slightly simplified models of the experimentally studied aluminium acetals in order to establish conformational preferences of the reagents that could help rationalising their experimental reactivity. Bromide, iodide and phenylselenide derivatives were investigated, with one, two, or no methyl substituents at the α-position.

As a result of its Lewis acid property, we made the assumption that the aluminium atom in the aluminium acetals is likely to be involved in Lewis acid/Lewis base interactions. Two Lewis bases are present in the reaction medium, namely the halide (or chalcogenide) and the second oxygen atom. Both intramolecular and intermolecular interactions can be considered. Since we suspected steric hindrance to play a significant role in the mode of complexation, we chose to keep, in the theoretical model, two bulky isobutyl groups on the aluminium atom, as well as a secondary alcohol unit. The chiral allylic alcohol moiety used in the experimental study was substituted with an isopropyl group in order to minimise the number of conformers and diastereoisomers to be modelled (Figure 1). The analysis revealed two series of conformers in the mono-

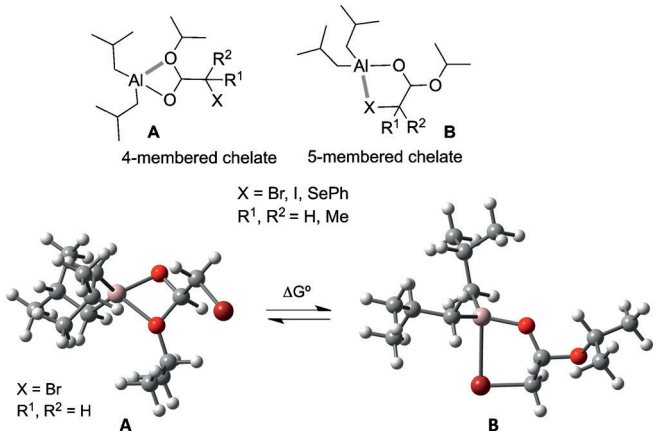

Figure 1. Possible conformations for the aluminium acetals at the PCM(toluene)-B3LYP/6-31 + G(d,p) level.

meric structures, showing an intramolecular interaction between the aluminium atom and either the second oxygen atom (Figure 1, structure **A**) or the halide/chalcogenide atom (Figure 1, structure **B**).[9]

The distribution between the four- and five-membered chelates is dependent on the halide (chalcogenide) atom. If no methyl substituent is located at the α-position, the bromide and selenide derivatives strongly favour the Al···X interaction (conformer **B**), the resultant stabilisation leading to almost 100% of such conformers (Table 6, entries 1 and 7). This preference for the Al···X interaction also applies for the corresponding monomethylated derivatives (Table 6, entries 2 and 8). In contrast, the related iodine derivatives strongly favour the Al···O interaction (conformer **B**) for both the non-methylated and the monomethylated derivatives (Table 6, entries 4 and 5). Finally, the Al···X interaction (X = Br, I, PhSe) was found to be favoured for the more sterically hindered dimethylated derivatives, regardless the nature of the X atom (Table 6, entries 3, 6 and 9). In these cases, the intramolecular Al–X distances are slightly shorter than those in the non-methylated and monomethylated derivatives.

Table 6. Distribution of the 4-membered vs. 5-membered chelates in the aluminium acetal structures (PCM(toluene)-B3LYP/6-31+G(d,p) level at 195 K).

Entry	Halide X	R^1	R^2	ΔG° [kcal mol^{-1}][a]	**B**[b]	dAl-X[c]
1	Br	H	H	+1.94	99.7	2.74
2	Br	Me	H	+2.15	99.9	2.77
3	Br	Me	Me	+3.23	>99.9	2.70
4	I	H	H	−2.46	0.2	3.24
5	I	Me	H	−1.03	13.3	3.09
6	I	Me	Me	+0.67	92.7	3.04
7	PhSe	H	H	+5.47	>99.9	2.67
8	PhSe	Me	H	+7.77	>99.9	2.67
9	PhSe	Me	Me	+7.22	>99.9	2.66

[a] Gibbs energy difference between the most stable conformers **A** and **B**. [b] Sum of the relative population calculated at 195 K for the various conformers (see Experimental Part for details). [c] Length in Å.

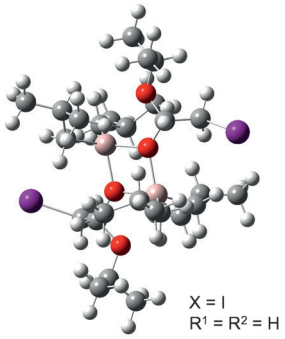

Figure 2. Example of dimeric structure of aluminium acetals (X = I; $R^1 = R^2 = H$) at the PCM(toluene)-B3LYP/6-31+G(d,p) level.

Table 7. Gibbs free energy of dimerisation ΔG° of non-methylated, monomethylated and dimethylated aluminium acetals, at the PCM(toluene)-B3LYP/6-31+G(d,p) level.

Entry	Halide X	R^1	R^2	ΔG° [kcal mol^{-1}]
1	Br	H	H	−15.49
2	Br	Me	H	−8.99
3	Br	Me	Me	+4.78
4	I	H	H	−6.33
5	I	Me	H	−7.00
6	I	Me	Me	+8.00
7	PhSe	H	H	−5.62
8	PhSe	Me	H	−2.65
9	PhSe	Me	Me	+11.76

In the case of simpler and thermally stable aluminium alkoxides, numerous dimeric structures have been reported previously (157 dimeric structures in the 2015 version of the Cambridge Structural Database).[10] As a consequence, it appeared necessary to consider such dimeric structures for the thermally unstable α-haloaluminium acetals.[11] Energy minima were located for the dimeric structures with a four-membered Al_2O_2 ring, regardless the initial conformation (structure **A** or **B**) of the monomeric species (Figure 2).[9c] This allowed us to calculate the Gibbs free energies (ΔG°) of the dimerisation for different aluminium acetals.

The results presented in Table 7 clearly indicate that the dimerisation processes from monomeric aluminium acetals are exergonic reactions for the least sterically hindered aluminium acetals, those presenting none, or only one methyl substituent at the α-position. In these cases, dimeric structures are favoured on the grounds of thermodynamics, regardless of the nature of the halide or chalcogenide. However, significant differences in energy have been calculated depending on the nature of the X group (X = Br, I, PhSe). For instance, the dimerisation process appeared to be much more favourable for the non-substituted α-bromo aluminium acetal, than for the corresponding iodo- and phenylselenyl derivatives (Table 7, entries 1, 4 and 7). Although less pronounced, this trend is still followed for the monomethylated aluminium acetals (Table 7, entries 2, 5 and 8). At this stage, despite favourable orientation in the optimised structures, the participation of the halide to form dimeric oxygen-bridged structures with a five-coordinate aluminium centre[9a,10c] could be ruled out. Indeed, the distance between the aluminium and the halogen atoms in the dimers appeared to be significantly longer than those observed in the monomers.

By contrast, α,α-dimethylated aluminium acetals appeared to be less stable in the dimeric than in the monomeric form (Table 7, entries 3, 6 and 9)[12] and this is consistent with the increase in steric hindrance on the surroundings of the aluminium atom. Other hypotheses (six- and eight-membered chelates) seemed to be unstable, as none of the optimised geometries converged to these structures, but rather to the previous four-membered chelates. Trimeric structures were not considered for these species as they seem very unlikely due to steric hindrance,[13] and the presence of dialkylaluminium derivatives (and not trialkoxides species).[14]

Determination of the structure by NMR spectroscopy

The DFT methods gave us good indication that different types of structures could be expected depending on the nature of the substituents of the aluminium acetals. Of course, the thermodynamic criterion is insufficient to guarantee the presence of dimers in solution under our reaction conditions. Indeed, considering the highly crowded environment at the aluminium atom, the dimerisation process, although favoured thermodynamically for some substrates, might be kinetically beyond reach at low temperature. Consequently, we considered the possibility of accessing the structure of the aluminium acetals using diffusion-ordered NMR spectroscopy (DOSY) experiments at low temperature. Diffusion-ordered spectroscopy of various nuclei (e.g., ^{1}H, ^{13}C, ^{6}Li, ^{31}P) proved to be extremely useful for the determination of the aggregation state of lithiated species.[15] We hoped that ^{13}C-INEPT DOSY with internal references[15c,16] would allow us to determine the aggregation state of the different species in solution. The first step of this study was to measure ^{1}H and ^{13}C spectra of the aluminium acetals resulting from the reduction of α-haloesters with DIBAL-H. For the sake of simplicity in the analysis of the ^{13}C spectra, ^{13}C-labelled α-haloesters (enriched at the carbonyl group) were prepared.[17] The ^{13}C NMR spectra were measured with delays allowing for quasi-quantitative experiments.

The synthesis of ^{13}C-labelled compounds that could be used in this study as an internal reference system were undertaken, keeping in mind that these references should be easy to access and should not interact with the different aluminium species in solution (aluminium acetals, DIBAL-H). At the same time, these ^{13}C-labelled compounds should give characteristic signals in a region of the NMR spectrum free from other signals. We selected anisole derivatives, the Lewis base properties of which were expected to be low enough not to interact with the aluminium acetals (the latter proved to be unstable in THF solution, vide supra). The reduction of various α-haloesters was carried out at −73 °C in [D_8]toluene, using a commercially available solution of DIBAL-H in toluene, then the solution was rapidly transferred into the NMR sample, pre-cooled at −80 °C (see Supporting Information for details). The 1D (^{1}H, ^{13}C, Jmod) and 2D (^{13}C-INEPT DOSY) spectra were measured at −70 °C, the viscosity of the solution being too high at lower temperatures. The samples were measured in the absence and in the presence of internal references, to ensure that the anisole derivatives (see below) did not affect the stability of the aluminium acetal species. Moreover we verified that these anisole derivatives had no interaction with DIBAL-H, which would result in dramatic errors in the molecular weight of the species.

We decided then to prepare ^{13}C-labelled bromoesters, carry out the reduction with DIBAL-H and try to get an estimate of their molecular weight thanks to the diffusion ordered spectroscopy (^{13}C-INEPT DOSY). For the sake of simplification, we decided to introduce the enriched ^{13}C at the carbonyl group in the bromoester. This would make the synthesis of the precursor easier and we expected the signal for the ^{13}C corresponding to the acetal centre to appear in a region of the NMR spectrum almost free from other signals. The precursors **5a** and **5b** were prepared in one step from allyl alcohol and commercially available 1-^{13}C-bromoacetic acid (>99% ^{13}C) and 1-^{13}C-bromopropionic acid (>99% ^{13}C), respectively (Scheme 2a). The selenoester **5c** was prepared in two steps from 1-^{13}C-bromopropionic acid (Scheme 2b). Finally, *gem*-dimethyl bromoester **5d** was obtained in two steps from 1-^{13}C-2-methylpropionic acid (>99% ^{13}C) (Scheme 2c). Three ^{13}C-labelled internal standards were synthesised in 2–3 steps from commercially available 2,6-dibromoanisole (Scheme 2d).

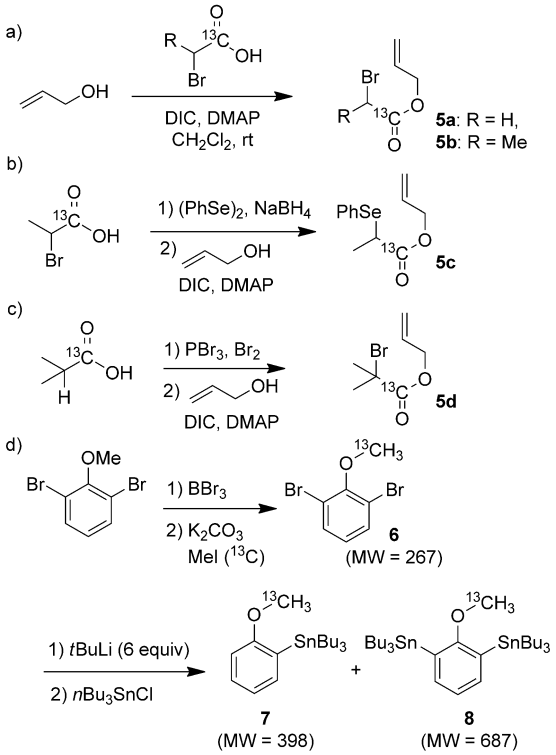

Scheme 2. Preparation of ^{13}C-labelled precursors **5a**–**d** and ^{13}C-labelled internal references **6**–**8**.

The reduction of **5a** was initially carried out with 1.2 equivalents of DIBAL-H (commercially available solution, 1.2 M in toluene) but for the rest of the study 2 equivalents of reducing agent were used to ensure complete reduction and to avoid any changes in the relative integration of the signals during the DOSY experiments that could be caused by the conversion of unreactive bromoester, thus introducing significant error in the determination of the molecular weight. Although changes in the structure have been observed for organoaluminium derivatives obtained from aminoacids depending on the reactant molar ratio,[9d,18] no changes in the ^{13}C NMR spectra were observed for the reduction of **5a** with 1.2 or 2 equivalents of DIBAL-H, suggesting the existence of the same species at both molar ratio. For practical convenience, the reduction of bromoester **5a** was then carried out in [D_8]-toluene at −73 °C with 2 equivalents of DIBAL-H (1.2 M in toluene) at a concentration slightly higher than those usually used in our experiments for the sequence reduction/radical cyclisation.[19] The solution was

then quickly transferred into a pre-cooled NMR tube and the ^{13}C spectrum of the reaction mixture was then measured (see Supporting Information for details). We were pleased to obtain a very clean ^{13}C NMR spectrum, which clearly indicated complete consumption of the starting material and formation of two new species, as indicated by the presence of two intense signals at 97.21 and 97.05 ppm (Figure 3), a region characteristic of the acetal carbon atom. Theoretical calculations of the ^{13}C NMR spectra estimate the chemical shift for the *C*(OR)OAl carbon atom to be in the region 100 ppm, while the corresponding aluminium alkoxides CH_2–OAl should appear near 70 ppm (see Supporting Information for details). The relative integration of the two signals gave an approximate 2:1 ratio for the two species. The presence of two signals is consistent with the presence of two diastereomeric dimeric species formed by the dimerisation of a chiral, racemic monomeric aluminium acetal in a moderately selective dimerisation process (Figure 4).[20]

The results of the INEPT ^{13}C-DOSY experiment allowed us to rule out the existence of monomeric species in solution for the non-substituted aluminium acetal derived from **5a**. A good calibration line ($y=7.2545x-67.36$, $r^2=0.99$) was established by plotting the logarithm of the molecular weight (MW) of the ^{13}C-labelled references (**6**, **7**, **8**, and [D_8]-toluene), versus the logarithm of their diffusion coefficient values measured from the ^{13}C INEPT-DOSY experiment (Figure 3). Diffusion coefficients values measured at 97.21 and 97.05 ppm led then, by extrapolation, to molecular weight consistent with dimeric species (see Supporting Information for details).

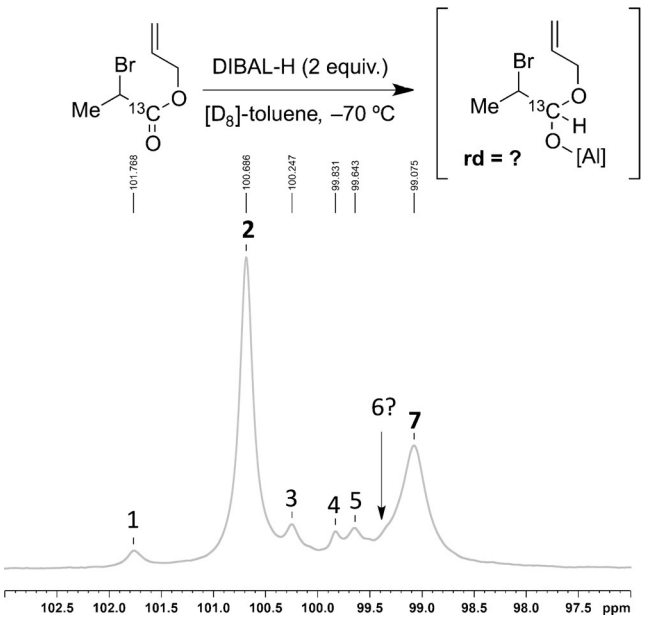

Figure 4. ^{13}C NMR spectrum of aluminium acetal derived from ^{13}C-labelled bromoester **5b**, measured at 203 K.

The reduction of monomethyl α-bromoester **5b** with DIBAL-H at −70 °C gave a more complex system. The aluminium acetal species could also be observed in the ^{13}C NMR spectrum, with characteristic signals in the region of 90–100 ppm. Here again, ^{13}C NMR spectrum with J-modulation of spin echo

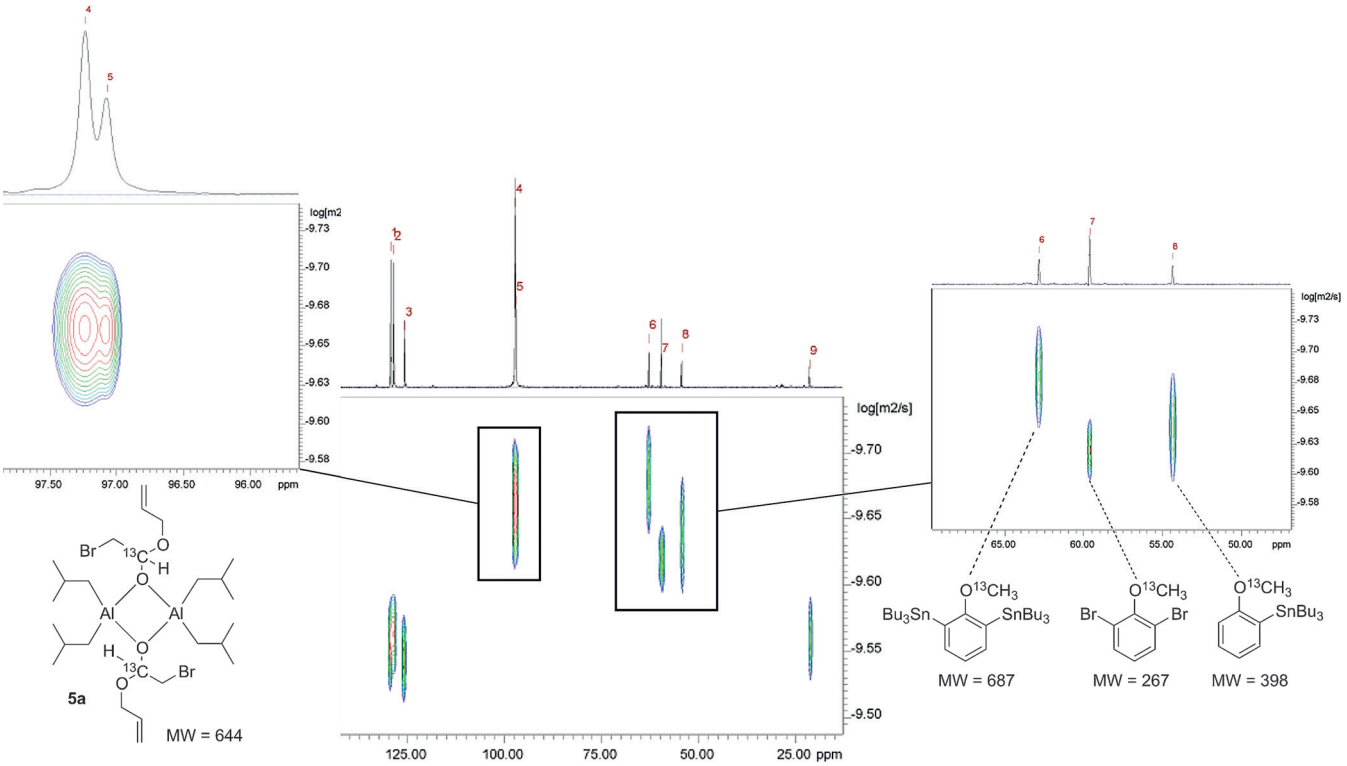

Figure 3. ^{13}C INEPT-DOSY of aluminium acetal derived from **5a**.

(Jmod) indicated that the signals present in this region corresponded to the ^{13}C-labelled *C*H (and not *C*H$_2$). The presence of (at least) six signals in the region 98–102 ppm tends to support the hypothesis of the diastereomeric dimeric structures for this monomethyl aluminium acetal, in agreement with the first-principle calculations. By comparison with the ^{13}C NMR spectrum obtained for the reduction of **5a**, for which a certain level of diastereoselectivity was observed for the dimerisation process (vide infra, relative integration ca. 2:1), the relative integration of the different signals (see peaks 2 and 7 in Figure 4) tends to indicate that the reduction of α-substituted bromoester **5b** proceeded with a high level of stereocontrol. Unfortunately, the complexity and the overlapping of ^{13}C signals in the range 98–102 ppm prevented an accurate estimation of the formula weights for each peak. However, the analysis of the ^{13}C INEPT-DOSY considering the global integration of the six (or seven) signals between 98 and 102 ppm led to a molecular weight of 460, which is intermediate between the theoretical molecular weights of the monomeric and dimeric species (see Supporting Information for details).

Heterodimeric structures **G** and **H** (Scheme 3) could be obtained by reaction between aluminium acetal **C** and aluminium alkoxide **F** and **D**, respectively. Both **D** and **F** result from the decomposition of the aluminium intermediate **C**, with **D** and **E** being the primary products and **F** being obtained by over-reduction of **E** with the excess of DIBAL-H. Although possible, the heterodimeric structures **G** and **H** have been ruled out in the case of monomethyl α-bromoester **5b**, because no intense signals characteristic for a –*C*H$_2$O(Al) species were observed in the region 70 ppm (**H** cannot be formed without other species (such as **G**) containing at least one ^{13}C-labelled *C*H$_2$O(Al) moiety being present). The homodimer (not shown) formed from the diisobutylaluminium alkoxide **D** would also be present if aluminium acetal **C** decomposed, but as it is not ^{13}C-labelled, the corresponding signal for the –*C*H$_2$O(Al) would be weak. More likely, heterodimer **I** (MW = 478), might contribute to the six (or seven) signals observed on the ^{13}C NMR spectrum of aluminium acetal derived from **5b**. The contribution of heterodimer **I** to the mixture of species, if possible, should depend on the initial stoichiometry between the reactants.

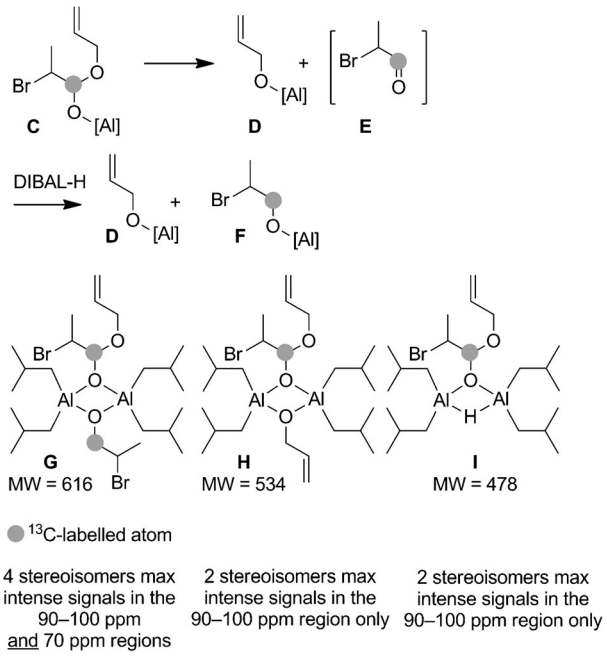

Scheme 3. Possible heterodimeric structures.

In contrast to the aluminium acetals derived from bromoesters **5a** and **5b**, we were unsuccessful in the preparation and observation of the aluminium acetal derived from selenoester **5c** (X = SePh). This failure is in agreement with the results obtained in the radical cyclisation of **1h**, for which a dramatic drop in the yield was observed between −73 °C and −40 °C (Table 4, entry 6 vs. Table 5, entry 9). It is likely that the rapid warm up during the transfer from the reaction flask led to the decomposition of the aluminium acetal formed in the reaction flask at −70 °C. The absence of experimental data, together with the moderate exothermicity of the dimerisation process calculated at the PCM(toluene)-B3LYP/6-31 + G(d,p) level (Table 7, entry 8) do not allow us to make conclusions concerning the aggregation state of aluminium acetals derived from α-substituted selenoesters. In other words, for these species, the existence of monomeric forms cannot be excluded. This, as we will see later, can have dramatic consequences on the diastereoselectivity of the radical cyclisation process.

Finally, we investigated the case of the challenging substrate **5d** (X = Br; $R^1 = R^2$ = Me). Because of its sterically crowded environment and the moderate yields obtained from **1i** in the radical cyclisation even at −73 °C (see Table 4, entry 10), it was expected that the observation of aluminium acetal species would be difficult. This was indeed the case and we obtained non-reproducible results. However, in one of our attempts at preparing the expected aluminium acetal species, we were able to observe a mixture between unreacted α-bromoester **5d**, an aluminium acetal species, and signals assigned to the aluminium alkoxide resulting from the over-reduction of **5d**. The observation of one main *C*H signal in the Jmod spectrum tends to support the presence of a monomeric structure for the aluminium acetal derived from α,α-disusbtituted bromoesters, in agreement with our calculations. However, at this stage a heterodimeric structure similar to dimer **I** (see Scheme 3) cannot be definitely ruled out.

With these experimental and theoretical data in hand, we started to investigate the energy profiles for the radical cyclisation and located transition states for the different cases.

Transition states for the radical cyclisation

Aluminium acetals are potentially reactive species by one of their oxygen atoms, the aluminium alkoxide moiety being nucleophilic enough to react with an acylating agent and to form mixed acetals.[21] Therefore, the reaction between non-cyclised or cyclised aluminium acetals and the tributyltin halide generated during the course of the reaction must be envisaged. In order to ensure that the species involved in the radical cyclisation step were truly aluminium acetals (and not tributyltin acetals), we carried out a ^{119}Sn NMR analysis of the crude reaction

mixture. This study clearly indicates the presence of Bu_3SnBr and Bu_6Sn_2 as the two major components of the reaction mixture, with very little amounts (if any) of tin alkoxide derivatives (see Supporting Information for details). We can conclude that, because no cyclic tin acetals were observed under these reaction conditions, it is very unlikely that linear tin acetal were formed to some extent as intermediates during the radical cyclisation process. Accordingly, only aluminium acetals will be considered as possible intermediates in the following calculations.

With this information in hand, and having established the structure for some of the aluminium acetals obtained during the reduction with DIBAL-H, we then turned our attention to the radical cyclisation itself. Two different cases have to be considered; the cyclisation of monomeric species and the cyclisation of dimeric species. In the case of dimeric aluminium acetals, the optimised geometries obtained at the PCM(toluene)-B3LYP/6-31+G(d,p) level showed that the halogen (or selenium) atom of the precursors for the radical cyclisation points outside of the structure, which makes them relatively accessible for abstraction by the tin-centred radical in a S_H2 homolytic substitution process.[22] Since these aluminium acetals have been proved to be more stable in a dimeric form and because these structures allow for halogen abstraction (X=Br, I) by the tin-centred radical to proceed with a nearly collinear approach, it appears unlikely that the radical cyclisation would require the aluminium acetal to rearrange into a monomeric structure prior to halogen abstraction in these cases. It seems even more unlikely that once the halogen atom abstraction has been achieved, the dimeric carbon-centred radical has enough time to collapse and give a monomeric structure before the 5-*exo*-trig cyclisation takes place. Accordingly, dimeric structures will be considered for the search of transition states for the radical cyclisation of non-methylated and monomethylated derivatives. The presence of the four isobutyl groups in the dimeric aluminium acetals makes the environment at the four-membered ring formed by the dimerisation process so crowded (see Figure 2) that the possibility of the two radical cyclisation that take place on the dimers to be correlated seems very unlikely. Instead, two totally independent radical cyclisation events are believed to take place in these structures. Accordingly, and for the sake of calculation cost, the search for transition states was carried out on the simplified systems depicted in Figure 5.

The case of monomeric aluminium acetals is more complex. Indeed, for the more hindered *gem*-dimethyl-substituted aluminium acetals, the favoured structure **B** implies complexation between the aluminium atom and the halogen (or chalcogen) atom. Although this mode of complexation results in a slightly longer carbon–halogen (or carbon–chalcogen) bond, thus suggesting a weakening of these bonds, the halogen (or chalcogen) abstraction might be disfavoured on structure **B** due to the presence of the bulky isobutyl groups on the aluminium atom. In this case, the halogen abstraction would probably deviate from the ideal attack angle, which was previously determined to be nearly collinear in the case of bromine and iodine (Figure 6).[23] The deviation from this ideal situation should result in an increase in the energy required to break this bond (not calculated). Accordingly, the halogen atom abstraction might be easier on either monomeric structures **A**, or on the least stable dimeric structures. At this point, we reasoned that the minor structure **A** is the reactive species in solution and, in this case a monomeric radical involving a four-membered chelate was considered.

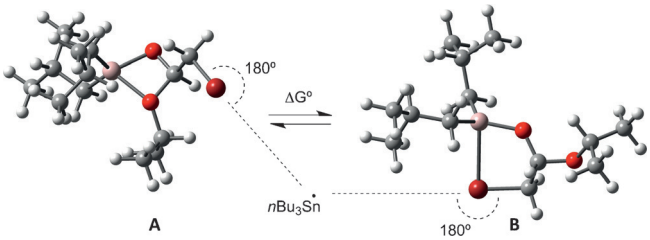

Figure 6. Halogen (chalcogen) abstraction by the tin-centred radical on monomeric aluminium acetals.

In contrast to the parent Ueno–Stork reaction, for which the stereoselectivity can be easily determined from the ratio of products, it was difficult to have access the diastereoselectivity of the radical cyclisation involving aluminium acetals. Indeed, in this case the aqueous work-up delivers a lactol, for which the hemiacetal centre is highly epimerisable. One alternative could be to trap the cyclic aluminium acetal to form a mixed acetal,[21] but both the reaction conditions for the trapping and the low stability of the resulting products (see below) would result in a lack of accuracy in the determination of the levels of stereoselectivity. For these reasons, we decided to compare the energy profiles of the radical cyclisation involving aluminium acetals with those involving α-bromoacetals (Ueno–Stork reaction). The comparison was made for both the 5-*exo*-trig and 5-*exo*-dig processes. Although calculations have already been reported by some of us[24] for the Ueno–Stork cyclisation onto carbon–carbon double bonds, for the sake of comparison these systems have been (re)computed at the BHandHLYP/6-311++G(d,p) level of theory to be consistent with the aluminium acetal models.

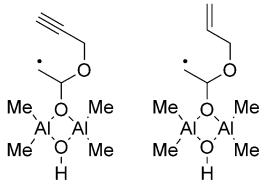

Figure 5. Structure used in the calculations to locate transition states for the radical cyclisation.

5-exo-dig Cyclisations for Ueno–Stork acetals and dimeric aluminium acetals

The search for transition states was systematically performed directly at the BHandHLYP level of theory with the basis set 6-311++G(d,p). For all optimised structures, frequency

calculations were performed to ascertain their nature (minima or transition states). A rapid conformational analysis was performed for both the transition states and minima in order to locate the most stable structures for each series.

Two pseudo-chair transition states were located for the 5-*exo*-dig Ueno–Stork cyclisation, the most stable presenting a pseudo-axial disposition for the OCH_3 group. This is in good agreement with the related 5-*exo*-trig Ueno–Stork cyclisations previously investigated by Schiesser and Renaud.[24] The most stable transition state ($\mathbf{TS_{UE}A}$) lies at $+7.5\ kcal\,mol^{-1}$ above the radical precursor (Gibbs free energy calculated at 195 K in the gas phase). The pseudo-equatorial transition state ($\mathbf{TS_{UE}B}$) appears about $2.9\ kcal\,mol^{-1}$ above $\mathbf{TS_{UE}A}$ (see Supporting Information for details). Similarly, two pseudo-chair transition states were located for the radical cyclisation of aluminium acetal derivatives onto a triple bond (Figure 7). The transition state $\mathbf{TS_{AA}A}$ ($+9.5\ kcal\,mol^{-1}$) with a pseudo-axial C–O(Al) bond is still more stable than transition state $\mathbf{TS_{AA}B}$ ($+9.8\ kcal\,mol^{-1}$) with a pseudo-equatorial C–O(Al) bond, but significantly more destabilised than for the corresponding Ueno–Stork acetal ($+7.5\ kcal\,mol^{-1}$). The much lower difference in energy between $\mathbf{TS_{AA}A}$ and $\mathbf{TS_{AA}B}$ compared to the corresponding Ueno–Stork cyclisation ($0.3\ kcal\,mol^{-1}$ vs. $2.9\ kcal\,mol^{-1}$ for the Ueno–Stork cyclisation) indicates that even at $-78\,^{\circ}C$, both transition states $\mathbf{TS_{AA}A}$ and $\mathbf{TS_{AA}B}$ do contribute to the formation of the cyclised compounds, a significant qualitative difference between the two reactions.

5-exo-trig Cyclisations for Ueno–Stork acetals and dimeric aluminium acetals

Cyclisation onto double bond was then studied. As previously, we conducted the analysis of the simple OCH_3 acetal used in the Ueno–Stork reaction. Four transition states were located at the BHandHLYP/6-311++G(d,p) level (see Supporting Information for details), namely pseudo-chair axial-*cis* $\mathbf{TS_{UE}C}$, twist axial-*trans* $\mathbf{TS_{UE}D}$, pseudo-chair equatorial-*cis* $\mathbf{TS_{UE}E}$, and equatorial-*trans* $\mathbf{TS_{UE}F}$. Here again, the results are consistent with published data,[24] and in agreement with the levels of diastereoselectivity observed for these types of radical cyclisation.[25]

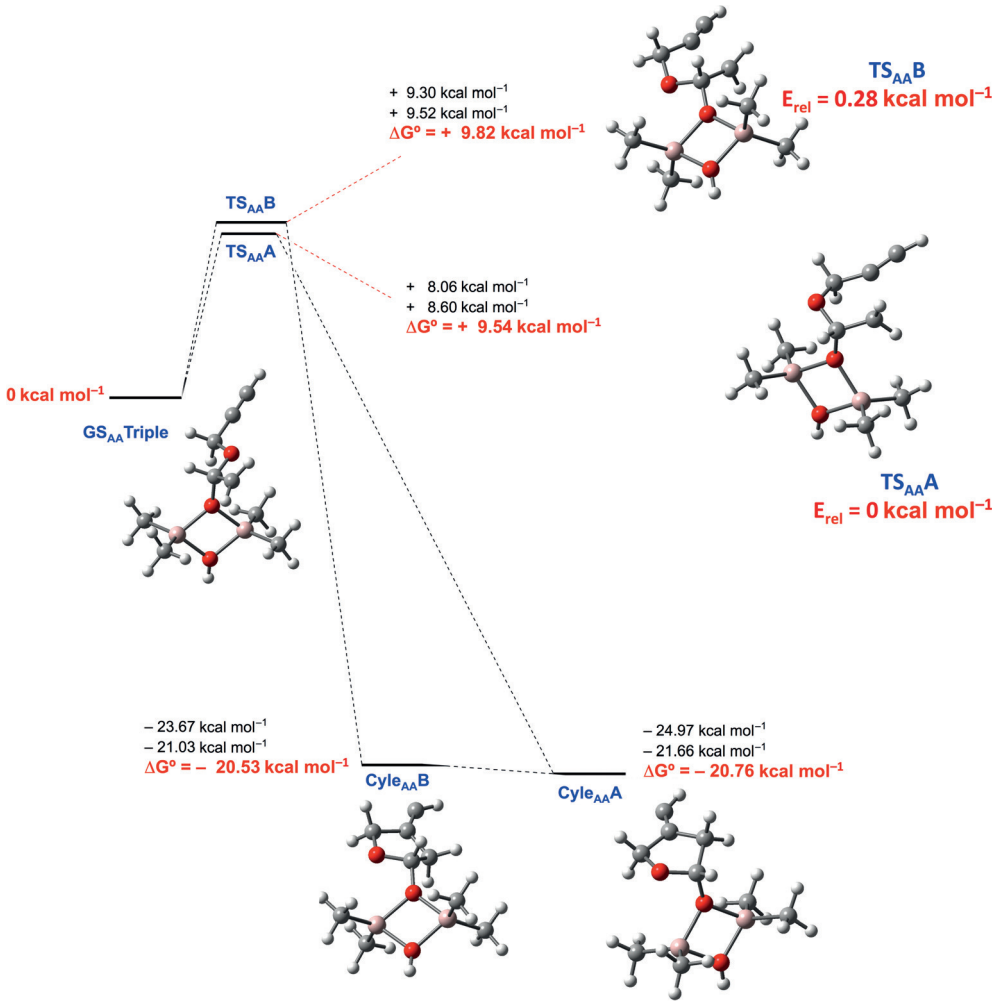

Figure 7. Energy profile for the radical 5-*exo*-dig cyclisation of aluminium acetals (BHandHLYP/6-311++G(d,p) level at 195 K). The values indicated on the energy profile refer to the difference in electronic energy ΔE (top), electronic + zero-point energy correction $\Delta(E+ZPE)$ (middle), and Gibbs free energy ΔG° (bottom, in red) with the uncyclised radical GS_{AA}Triple.

The two more stable transition state $TS_{UE}C$ and $TS_{UE}D$ present a pseudo-axial disposition of the OCH_3 group allowing for a better overlapping between the oxygen lone-pair and the σ^*_{C-O} bond (anomeric effect).[26] Transition states $TS_{UE}C$ and $TS_{UE}D$ were found 5.8 kcal mol^{-1} and 6.9 kcal mol^{-1}, respectively, above the reactants. The two pseudo-chair transition states $TS_{UE}E$ (+8.5 kcal mol^{-1}) and $TS_{UE}F$ (+10.7 kcal mol^{-1}) lead to cyclic acetals with the *trans* and *cis* relative configuration, respectively, but they are much more energetic than the most stable transition state $TS_{UE}C$ to contribute significantly to the diastereoselectivity of this cyclisation process. The thermochemical data calculated at 195 K indicated a 1.2 kcal mol^{-1} gap between $TS_{UE}C$ related to the *cis* isomer and $TS_{UE}D$ related to the *trans* one. The DFT energy profile was found consistent with the high levels of stereoselectivity observed at low temperature for 5-*exo*-trig Ueno–Stork cyclisations.

We then turned our attention to the determination of the energy profile for the related radical cyclisation of aluminium acetals. As mentioned previously, one of the issues here was the loss of the stereochemical information during the work-up of the reaction, due to the rapid epimerisation of the anomeric centre in the final lactol. Insights into stereoselectivity of the cyclisation process were sought by attempting to trap the cyclic aluminium acetal intermediate. The radical cyclisation was carried out with bromoester **5a** (not ^{13}C-labelled) under our standard reaction conditions, then the resulting cyclic aluminium acetal was trapped by benzoyl fluoride in the presence of pyridine and 4-dimethylaminopyridine (DMPA).[21c,d] These reaction conditions proved to give slightly better results in our case than the use of acetic anhydride, and cyclic acetal **9** was obtained in a modest 65% yield for the reaction carried out in toluene as a 66:34 mixture of diastereomers (Scheme 4). Slightly lower yield and selectivity were obtained in CH_2Cl_2 (41%, d.r. = 60:40). These diastereomeric ratios are to be considered with great care because on the one hand, modest yields were obtained both in toluene and methylene chloride and, on the other hand, the ratio were found to change during purification by flash chromatography over silica gel, probably due to the instability of the cyclic mixed acetals.[25a] Although it is difficult to conclude at this stage, and despite the yields for these trapping reactions, it seems that the *cis*/*trans* (or *trans*/*cis*) selectivity was significantly lower than that observed for the corresponding Ueno–Stork reaction. It is worth noting that only the radical cyclisation involving a dimeric structure for the aluminium acetal is consistent with the moderate level of stereoselectivity observed. Indeed, calculations performed with monomeric species predicted that the *trans* configuration should be strongly favoured in this case (vide infra).

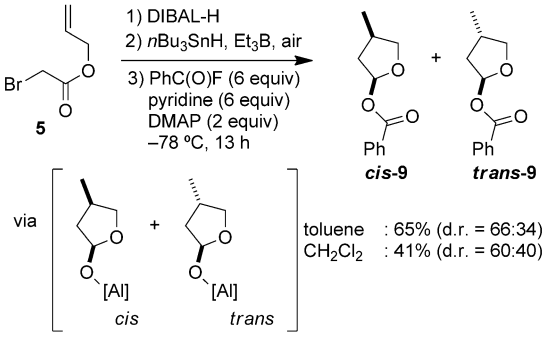

Scheme 4. Attempt at determining of the diastereoselectivity of the cyclisation process for aluminium acetals.

The energy profile for the 5-*exo*-trig cyclisation of aluminium acetals resembles that of the Ueno–Stork cyclisation, with two main differences: firstly, only pseudo-chair transition states were located and no twist conformation was found; secondly, the second more stable transition state $TS_{AA}D$ (leading to the *trans* isomer) is no longer having the alkoxide substituent in the pseudo-axial position (Figure 8). In contrast, it is a pseudo-chair transition state with the C–O(Al) bond in the pseudo-equatorial position, located only 0.3 kcal mol^{-1} above the most stable transition state $TS_{AA}C$, that leads to the *cis* isomer. The next higher transition states $TS_{AA}E$ (giving the *trans* isomer) and $TS_{AA}F$ (giving the *cis* isomer) were found 1.8 kcal mol^{-1} and 2.6 kcal mol^{-1}, respectively, above $TS_{AA}C$. These values are consistent with the low levels of stereocontrol that have been observed during the radical cyclisation of aluminium acetals. As previously noted for the 5-*exo*-dig cyclisation of aluminium acetal, the 5-*exo*-trig process for the aluminium acetal series showed a significantly higher activation barrier (1.6 times greater) than that of the corresponding Ueno–Stork cyclisation.

To further support the structure of the aluminium acetals, the hypothesis of a monomeric structure was investigated for the least hindered aluminium acetal. Three transition states were located for the cyclisation of monomeric aluminium acetals onto a C=C bond. $TS_{AA}G$ corresponding to the lowest activation barrier was found to lead to a cyclic aluminium acetal with a *trans* configuration (Figure 9). The two other transition states $TS_{AA}H$ and $TS_{AA}I$ both lead the *cis* isomer. The significant energy difference of 1.3 kcal mol^{-1} between monomeric transition states $TS_{AA}G$ and $TS_{AA}H$ (compared to 0.3 kcal mol^{-1} only in the hypothesis of dimeric structures, and 1.2 kcal mol^{-1} for the highly stereoselective Ueno–Stork cyclisation) suggests that a highly diastereoselective radical cyclisation could take place. These figures appeared to be inconsistent with the low stereoselectivity observed after trapping of the cyclic aluminium acetal with benzoyl fluoride. Altogether, the calculations made to determine the favoured structure of the starting bromoacetals, the low-temperature ^{13}C-INEPT DOSY experiments, the apparent diastereoselectivity of the cyclisation process on simple substrates and the DFT energy profiles converge to support the hypothesis of a dimeric structure for the aluminium acetals obtained from non-substituted α-bromoesters.

5-exo-dig and 5-exo-trig Cyclisations for monomeric, gem-dimethyl aluminium acetals

The energy profiles for the radical cyclisation of monomeric, *gem*-disubstituted aluminium acetals onto carbon–carbon

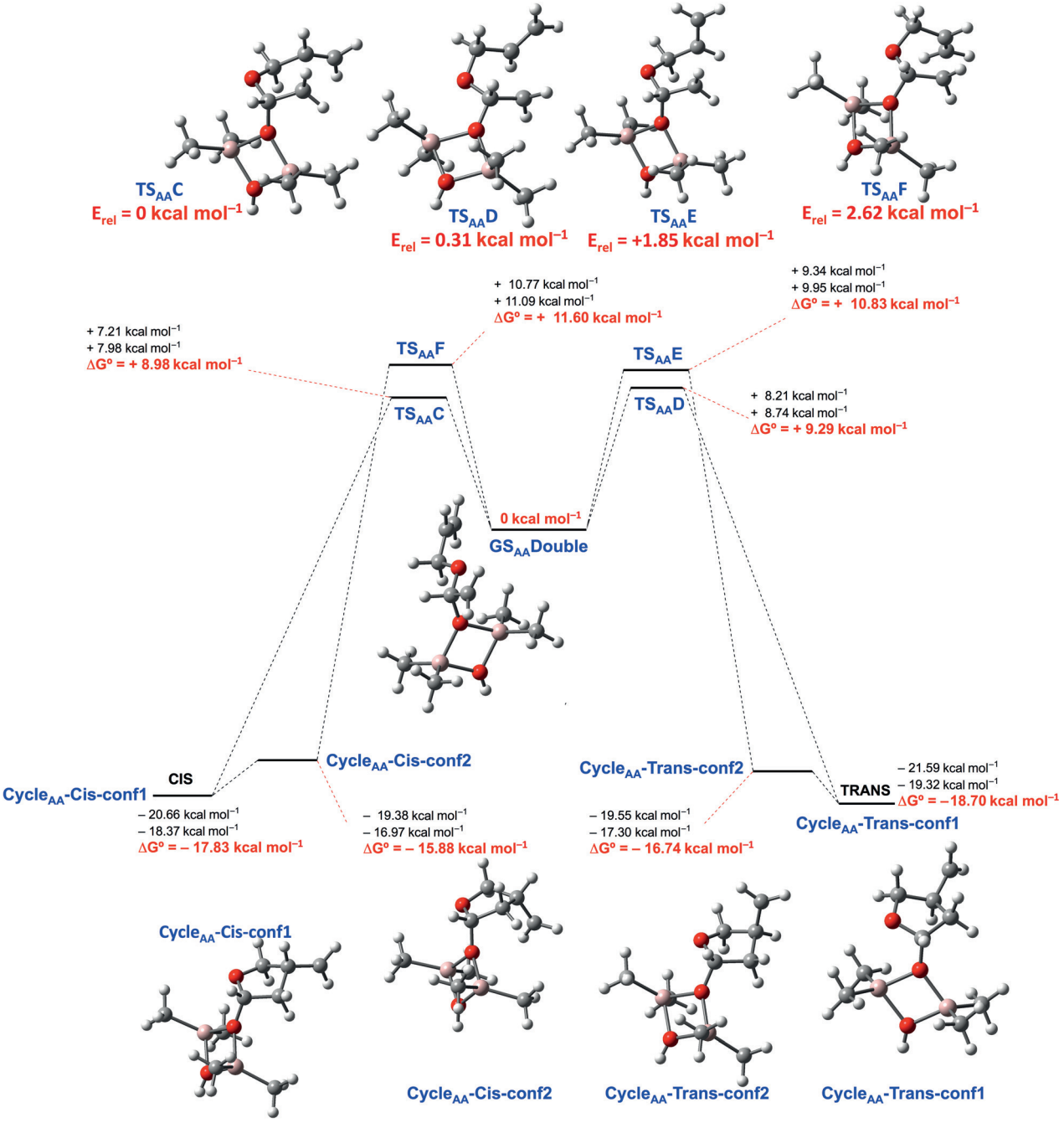

Figure 8. Energy profile for the radical 5-*exo*-trig cyclisation of aluminium acetals (BHandHLYP/6-311++G(d,p) level at 195 K). The values indicated on the energy profile refer to the difference in electronic energy ΔE (top), electronic + zero-point energy correction $\Delta(E+ZPE)$ (middle), and Gibbs free energy ΔG° (bottom, in red) with the uncyclised radical GS$_{AA}$Double. E_{rel} refers to the energy gap between the different transition states and most stable transition state **TS$_{AA}$C**.

triple and double bonds were calculated at the same level of theory as for the dimeric structures. Both in the cases of 5-*exo*-dig (Figure 10) and the 5-*exo*-trig cyclisation processes (Figure 11) the lowest activation barriers for the monomeric, *gem*-dimethyl aluminium acetals were found to be about 2.5–3.0 kcal mol^{-1} higher than those for the cyclisation of the corresponding non-substituted dimeric acetals. This tends to indicate that the radical cyclisation of monomeric, *gem*-dimethyl aluminium acetals is significantly more difficult than the corresponding cyclisation of dimeric non-substituted aluminium acetals. For the 5-*exo*-dig cyclisation process a single transition state **TS$_{AA}$J** (+12.6 kcal mol^{-1}) was located (Figure 10), while two transition states **TS$_{AA}$K** (+12.1 kcal mol^{-1}) and **TS$_{AA}$L** (+12.4 kcal mol^{-1}) were found for the 5-*exo*-trig cyclisation process (Figure 11). In the radical cyclisation onto a C=C bond, a slight preference for the formation of the cyclic aluminium

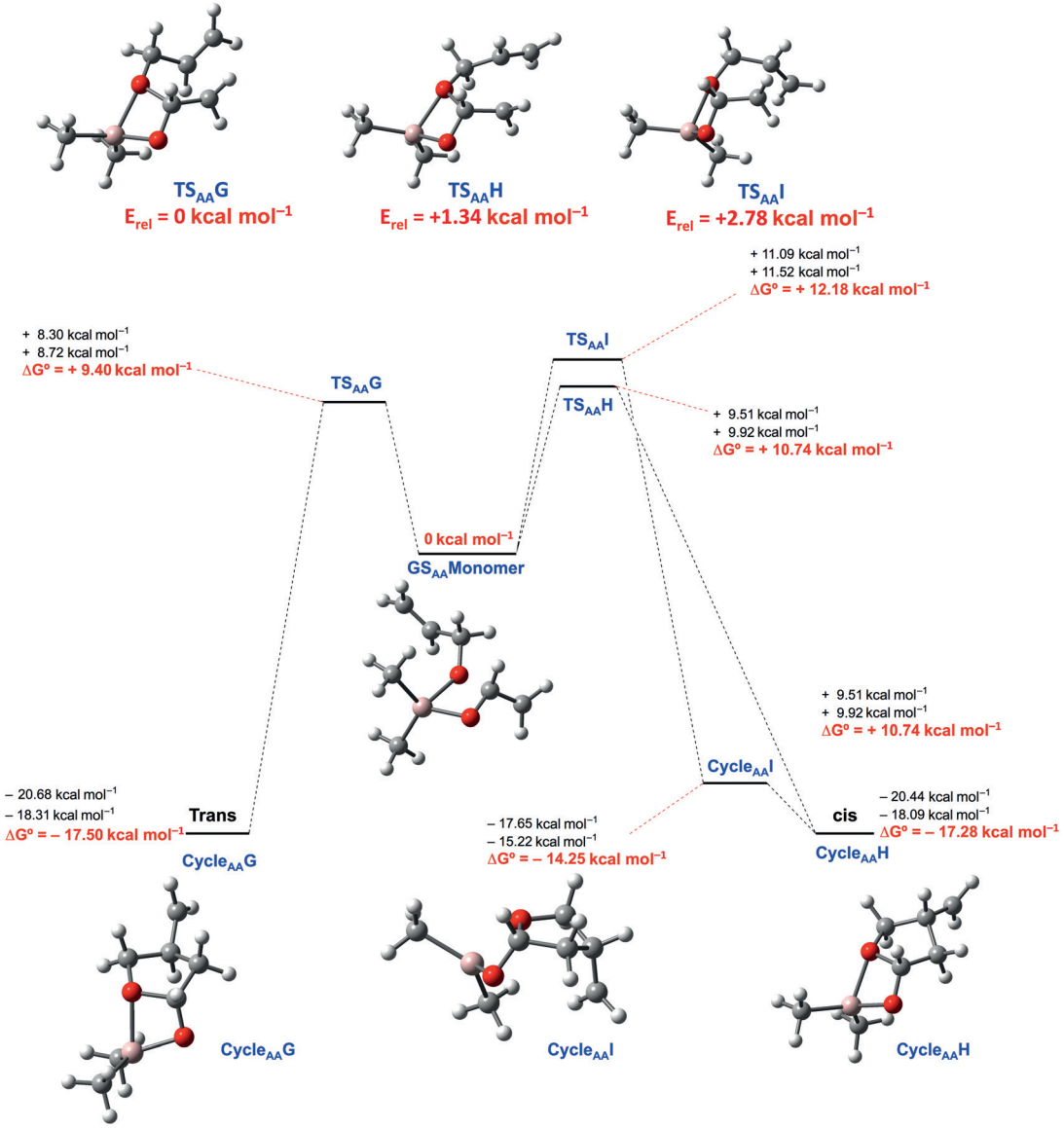

Figure 9. Energy profile for the 5-*exo*-trig cyclisation of non-substituted aluminium acetals with the hypothesis of a monomeric structure (BHandHLYP/6-311++G(d,p) level of theory at 195 K). The values indicated on the energy profile refer to the difference in electronic energy ΔE (top), electronic+zero point energy correction $\Delta(E+ZPE)$ (middle), and Gibbs free energy ΔG° (bottom, in red) with the uncyclised radical GS_{AA}Monomer. E_{rel} refer to the energy gap between the different transition states and most stable transition state **TS_{AA}G**.

acetal with the *trans* configuration was observed (0.2 kcal mol^{-1} between **TS_{AA}K** and **TS_{AA}L**).

Conclusion

The structure and the reactivity of aluminium acetals derived from α-haloesters have been studied in detail. Experimental data indicate that both the nature of the halide (or chalcogenide) and the substitution at the α-position play a key role in the stability of the tetrahedral intermediates and/or in the efficiency of the radical cyclisation. Various initiators were tested, together with various reducing agents and solvents. The best conditions for the ionic reduction/radical cyclisation sequence consist in the use of DIBAL-H as the hydride donor, with toluene or methylene chloride as solvent. Notably, some solvent effects have been observed with mono-substituted aluminium acetals depending on the nature of the halide. Among the initiators used in this study, diethylzinc, triisobutylaluminium and triethylborane were found to give good results. In the absence of any additional initiator, the radical reaction was also found to take place but the moderate yields obtained in this case suggest that the presence of oxygen might lead to a change in the structure of the tetrahedral intermediates into less stable aluminium acetal species. Low-temperature ^{13}C-INEPT DOSY NMR experiments allowed us to gain insights into the structures of these aluminium species and, together with DFT methods, to propose two different structures depending on the nature of the aluminium acetal considered. Both the

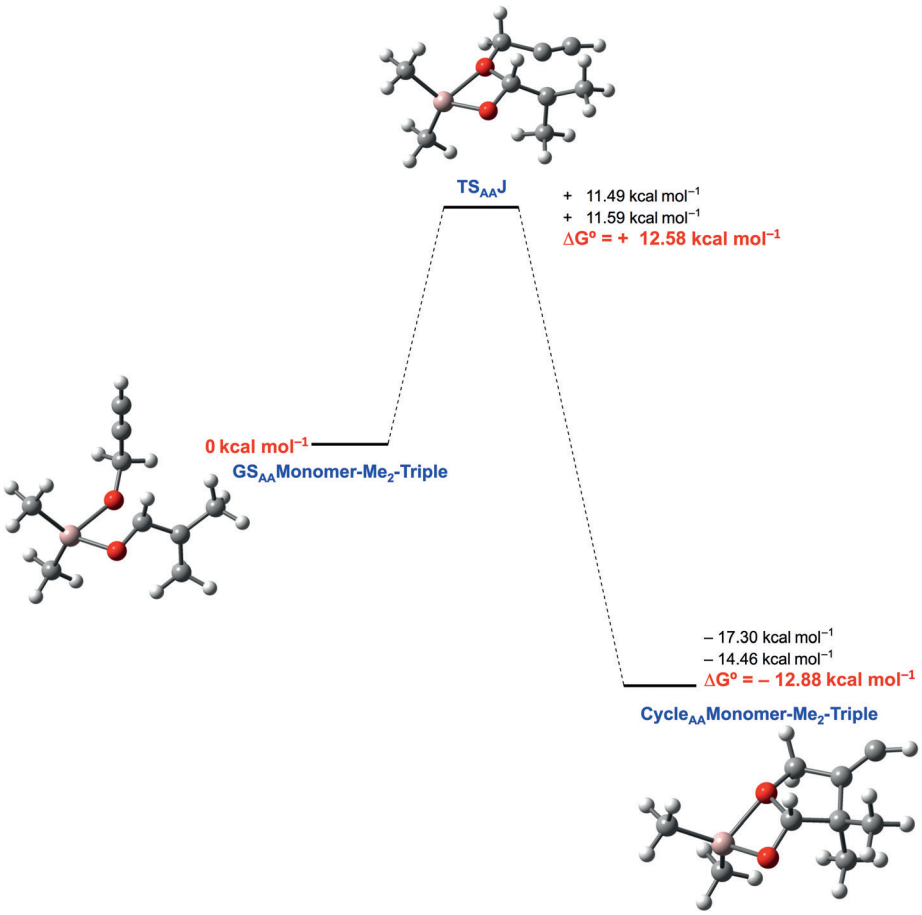

Figure 10. Energy profile for the radical 5-*exo*-dig cyclisation of monomeric, *gem*-dimethylaluminium acetals (BHandHLYP/6-311 + +G(d,p) level at 195 K). The values indicated on the energy profile refer to the difference in electronic energy ΔE (top), electronic + zero-point energy correction $\Delta(E+ZPE)$ (middle), and Gibbs free energy ΔG° (bottom, in red) with the uncyclised radical GS_{AA}-monomer-Me_2-Triple.

nature of the halide (or chalcogenide) and the substitution at the α-position proved to play a role, with dimeric structures with a four-membered chelate being preferred for the non-substituted aluminium acetals, while monomeric structures proved to be more stable for *gem*-dimethyl-substituted aluminium acetals. Energy profiles for the radical cyclisation (5-*exo*-dig and 5-*exo*-trig processes) were calculated at the BHandHLYP/6-311 + +G(d,p) level of theory and compared to the energy profiles for the Ueno–Stork cyclisation modelled at the same level of theory. Strong differences were observed between the two types of cyclisations, with the Ueno–Stork cyclisation being predicted to be much more stereoselective and presenting significantly lower activation barriers. Beside the two extreme cases (non-substituted and *gem*-disubstituted aluminium acetals), the DFT calculations also indicated the presence of dimeric structures for the mono-substituted aluminium acetals. This was confirmed by low-temperature NMR experiments. The latter also suggested a high level of diastereoselectivity for the reduction of α-bromoesters with DIBAL-H.

Acknowledgements

The authors thank the "Ministère de la Recherche et de l'Enseignement Supérieur" (MESR grant for A.B.) and the "Agence Nationale de la Recherche" (grant ANR-10-JCJC-0712 "Radic[Al]" for R.B., and ANR Blanc 13 BS07-0010-01 "UZFul-Chem" for J.-C.R.) for funding. F.D and R.B. thank Drs. J. Maddaluno, A. Harrison-Marchand and M. Durandetti (COBRA, Rouen) for helpful discussions and for offering access to the facilities for the preparation of the aluminium acetals used in for the NMR study. F.D. warmly acknowledges the Australian research council and the University of Melbourne for financial support and access to calculation facilities. D.J. acknowledges the European Research Council (ERC) and the Région des Pays de la Loire for financial support in the framework of a Starting Grant (Marches 278845) and the LumoMat Project, respectively. This research used resources of 1) the GENCI-CINES/IDRIS, 2) CCIPL (Centre de Calcul Intensif des Pays de Loire), and 3) a local Troy cluster.

Keywords: aluminium acetals · computational methods · NMR spectroscopy · radical cyclisation · reaction mechanisms

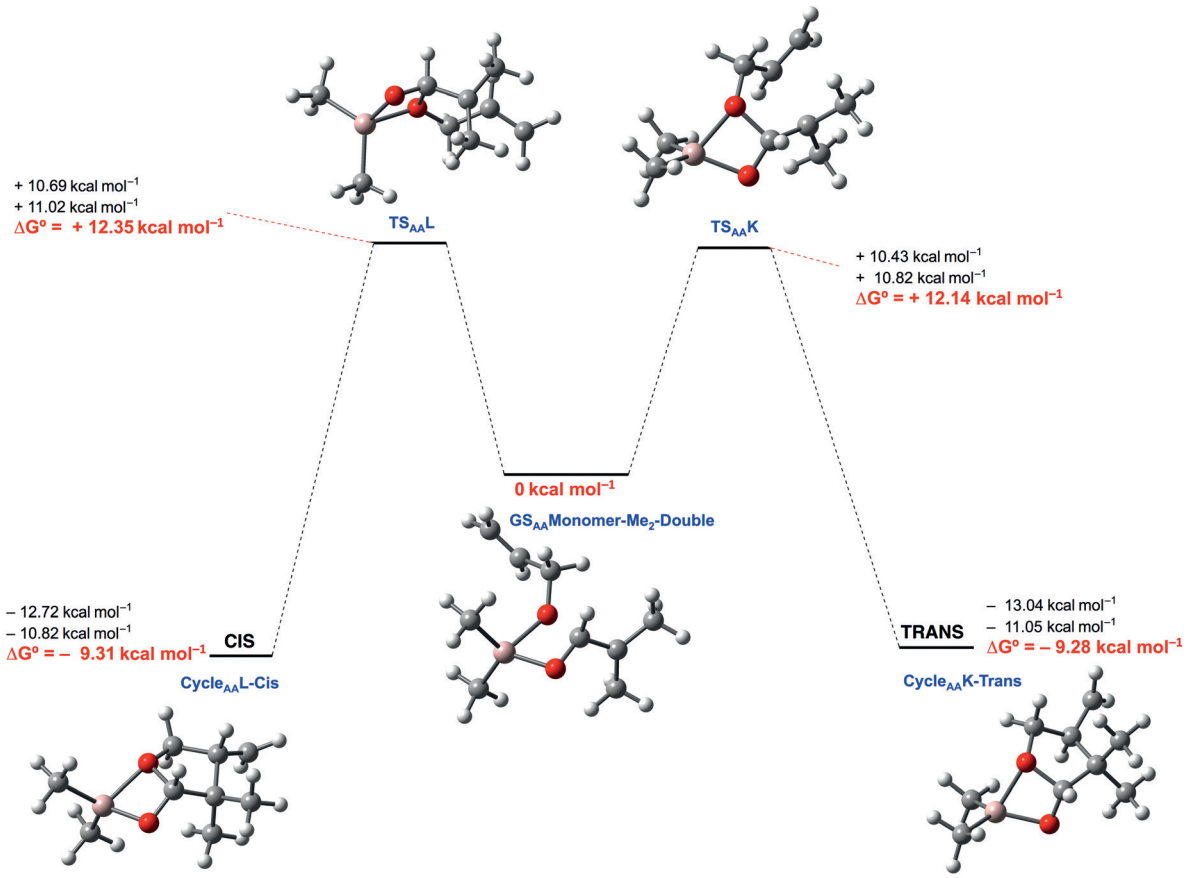

Figure 11. Energy profile for the radical 5-*exo*-trig cyclisation of monomeric, *gem*-dimethylaluminium acetals (BHandHLYP/6-311++G(d,p) level at 195 K). The values indicated on the energy profile refer to the difference in electronic energy ΔE (top), electronic+zero-point energy correction $\Delta(E+\mathrm{ZPE})$ (middle), and Gibbs free energy ΔG° (bottom, in red) with the uncyclised radical GSAA-monomer-Me_2-Double.

[1] For a review on the reactivity of aluminium acetals, see: A. Boussonnière, R. Bénéteau, J. Lebreton, F. Dénès, *Eur. J. Org. Chem.* **2013**, 7853–7866.
[2] A. Boussonnière, F. Dénès, J. Lebreton, *Angew. Chem. Int. Ed.* **2009**, *48*, 9549–9552; *Angew. Chem.* **2009**, *121*, 9713–9716.
[3] A. Boussonnière, R. Bénéteau, N. Zimmermann, J. Lebreton, F. Dénès, *Chem. Eur. J.* **2011**, *17*, 5613–5627.
[4] a) Y. Ueno, K. Chino, M. Watanabe, O. Moriya, M. Okawara, *J. Am. Chem. Soc.* **1982**, *104*, 5564–5566; b) Y. Ueno, K. Chino, M. Watanabe, O. Moriya, M. Okawara, *J. Chem. Soc. Perkin Trans. 1* **1986**, 1351–1356; c) G. Stork, R. Mook, Jr., S. A. Biller, S. D. Rychnovsky, *J. Am. Chem. Soc.* **1983**, *105*, 3741–3742; d) G. Stork, P. M. Sher, *J. Am. Chem. Soc.* **1983**, *105*, 6765–6766; e) G. Stork, P. M. Sher, *J. Am. Chem. Soc.* **1986**, *108*, 303–304; f) G. Stork, P. M. Sher, H.-L. Chen, *J. Am. Chem. Soc.* **1986**, *108*, 6384–6385; g) G. Stork, *Bull. Chem. Soc. Jpn.* **1988**, *61*, 149–154.
[5] For a review, see: X. J. Salom-Roig, F. Dénès, P. Renaud, *Synthesis* **2004**, 1903–1928.
[6] R. Bénéteau, J. Lebreton, F. Dénès, *Chem. Asian J.* **2012**, *7*, 1516–1520.
[7] R. Bénéteau, C. F. Despiau, J.-C. Rouaud, A. Boussonnière, V. Silvestre, J. Lebreton, F. Dénès, *Chem. Eur. J.* **2015**, *21*, 11378–11386.
[8] J. Lewiński, J. Zachara, P. Gos, E. Grabska, T. Kopec, I. Madura, W. Marciniak, I. Prowotorow, *Chem. Eur. J.* **2000**, *6*, 3215–3227.
[9] For examples of dialkylaluminium five-membered chelates derived from aminoacids, whose structure have been determined by X-ray diffraction studies, see: a) R. Kumar, M. L. Sierra, J. P. Oliver, *Organometallics* **1994**, *13*, 4285–4293; b) T. Gelbrich, E. Hecht, K. H. Thiele, J. Sieler, *J. Organomet. Chem.* **2000**, *595*, 21–30; c) J. F. Allan, W. Clegg, M. R. J. Elsegood, K. W. Henderson, A. E. McKeown, P. H. Moran, I. M. Rakov, *J. Organomet. Chem.* **2000**, *602*, 15–23; d) J. Lewiński, I. Justyniak, J. Zachara, E. Tratkiewicz, *Organometallics* **2003**, *22*, 4151–4157.
[10] F. H. Allen, *Acta Crystallogr. Sect. B* **2002**, *58*, 380–388. For some examples of aluminium alkoxides with a planar Al_2O_2 ring, see: a) T. Mole, *Aust. J. Chem.* **1966**, *19*, 373–379; b) B. Cetinkaya, P. B. Hitchcock, H. A. Jasim, M. F. Lappert, H. D. Williams, *Polyhedron* **1990**, *9*, 239–243; c) A. Pietrzykowski, T. Skrok, S. Pasynkiewicz, M. Brzoska-Mizgalski, J. Zachara, R. Anulewicz-Ostrowska, K. Suwinska, L. B. Jerzykiewicz, *Inorg. Chim. Acta* **2002**, *334*, 385–394; d) S. Szumacher, A. R. Kunicki, I. Madura, J. Zachara, *J. Organomet. Chem.* **2003**, *682*, 196–203; e) S. Yoon, S. H. Kim, J. Heo, Y. Kim, *Inorg. Chem. Commun.* **2013**, *29*, 157–159.
[11] The formation of dimeric aluminium species obtained by addition of diethylaluminium benzenethiolate onto aldehydes has been suggested on the basis of ^{13}C NMR analyses, see: G. Bastug, S. Dierick, F. Lebreux, I. E. Marko, *Org. Lett.* **2012**, *14*, 1306–1309.
[12] For examples of monomeric, sterically hindered aluminium alkoxides, see: M. D. Healy, D. A. Wierda, A. R. Barron, *Organometallics* **1988**, *7*, 2543–2548.
[13] Only very small aluminium alkoxides such as Me_2AlOMe have been reported to exist as trimeric structures, see: a) D. A. Drew, A. Haaland, J. Weidlein, *Z. Anorg. Allg. Chem.* **1973**, *398*, 241–248; b) A. Haaland, O. Stokkeland, *J. Organomet. Chem.* **1975**, *94*, 345–352.
[14] J. Pauls, B. Neumüller, *Z. Anorg. Allg. Chem.* **2000**, *626*, 270–279.
[15] a) I. Keresztes, P. G. Williard, *J. Am. Chem. Soc.* **2000**, *122*, 10228–10229; b) D. Li, C. Sun, P. G. Williard, *J. Am. Chem. Soc.* **2008**, *130*, 11726–11736; c) D. Li, R. Hopson, W. Li, J. Liu, P. G. Williard, *Org. Lett.* **2008**, *10*, 909–911; d) G. Kagan, W. Li, R. Hopson, P. G. Williard, *Org. Lett.* **2009**, *11*, 4818–4821; e) A. Botana, P. W. A. Howe, V. Caër, G. A. Morris, M. Nilsson, *J. Magn. Reson.* **2011**, *211*, 25–29.
[16] D. Li, I. Keresztes, R. Hopson, P. G. Williard, *Acc. Chem. Res.* **2009**, *42*, 270–280.
[17] C. Su, R. Hopson, P. G. Williard, *J. Org. Chem.* **2013**, *78*, 11733–11746.

[18] J. Lewiński, I. Justyniak, P. Horeglad, E. Tratkiewicz, J. Zachara, Z. Ochal, *Organometallics* **2004**, *23*, 4430 – 4437.
[19] Note: We have checked that no change in the NMR spectrum was observed for the reduction of **5a** at the concentration used in the radical cyclisation.
[20] The (*R*,*S*) dimeric structure for Table 6, entry 1 was found to be about 1.2 kcal mol^{-1} less stable than the corresponding (*R*,*R*) dimer in DFT calculations. Despite the fact that the potential energy surfaces have clearly not been explored, it rationalise the presence of two different species in solution in a ratio that deviates from 1:1.
[21] a) D. J. Kopecky, S. D. Rychnovsky, *J. Org. Chem.* **2000**, *65*, 191 – 198; b) D. J. Kopecky, S. D. Rychnovsky, *Org. Synth.* **2003**, *80*, 177 – 183; c) N. Sizemore, S. D. Rychnovsky, *Org. Synth.* **2012**, *89*, 143 – 158; d) Y. Zhang, T. Rovis, *Org. Lett.* **2004**, *6*, 1877 – 1879.
[22] a) J. E. Lyons, C. H. Schiesser, *J. Chem. Soc. Perkin Trans. 2* **1992**, 1655 – 1656; b) C. H. Schiesser, B. A. Smart, *Tetrahedron* **1995**, *51*, 6051 – 6060.
[23] C. H. Schiesser, B. A. Smart, T.-A. Tran, *Tetrahedron* **1995**, *51*, 3327 – 3338.
[24] O. Corminboeuf, P. Renaud, C. H. Schiesser, *Chem. Eur. J.* **2003**, *9*, 1578 – 1584.
[25] a) A. L. J. Beckwith, D. M. Page, *J. Org. Chem.* **1998**, *63*, 5144 – 5153; b) F. Villar, P. Renaud, *Tetrahedron Lett.* **1998**, *39*, 8655 – 8658; c) F. Villar, O. Equey, P. Renaud, *Org. Lett.* **2000**, *2*, 1061 – 1064; d) F. Villar, T. Kolly-Kovac, O. Equey, P. Renaud, *Chem. Eur. J.* **2003**, *9*, 1566 – 1577.
[26] The preference for the pseudo-axial position is in contradiction with the classical model for 5-*exo*-trig radical cyclisations, see: a) A. L. J. Beckwith, C. H. Schiesser, *Tetrahedron* **1985**, *41*, 3925 – 3941; b) D. C. Spellmeyer, K. N. Houk, *J. Org. Chem.* **1987**, *52*, 959 – 974.

Received: November 26, 2015
Published online on February 18, 2016